Primordial Probe: The Oldest Star of the Galaxy as a Dark Matter Laboratory

Diogo Coutinho

Abstract

In this thesis, I report the constraints on the properties of Higgs-like supersymmetric dark matter (DM) particles, by studying the evolution of the Population-II star SDSS J102915+172927 (Caffau's Star). It will be shown that this type of DM affects the internal structure of these stars through the energy released in the annihilation of DM particles that have accumulated in the star's core during its evolution. In some cases, the DM produces strong modifications on the present day stellar observables, such as the effective temperature and the surface gravity of the star. Accordingly, I have found that the DM density of the primordial halos where Population II stars were formed cannot be larger than 10^9 GeV cm^{-3}. Moreover, from the comparison of theoretical stellar predictions and observational data, I found that the DM (spin-dependent and spin-independent) scattering cross sections with baryons are smaller than 10^{-39} cm^2 and 10^{-42} cm^2, respectively. These predictions are consistent with the current limits of DM experimental direct detections.

1 Introduction

Dark matter (DM) makes for most of the matter content of the Universe. DM is believed to play a central role in the formation of structure in the Universe, like stars, galaxies and galaxy clusters. During the first stages of the primitive Universe, possibly prior to the baryogenesis occurs the production of DM particles. Later on these DM particles will form the gravitational web where the accretion of baryons will generate the first stars and galaxies. However, for all its importance, even after more than 80 years since the first observational evidence of DM in the Coma cluster by Zwicky, the particle properties of DM remains unknown. DM continues to be one of the leading open problems in modern physics (e.g. Bertone 2010).

In the last decade, many direct and indirect detection experiments entered in operation to search for this DM particle, which is expected to be a weakly interacting massive particle (WIMP). In a continuous manner, the majority of these experiments excluded a large part of the DM parameter space: DM particle mass – DM scattering cross sections with baryon nuclei (e.g., Panci 2014, and references therein). Recent results of DM direct detection experiments have created an unclear and confusing landscape, with positive signals coming from experiments such as DAMA, CoGeNT, CRESST-II and CDMS-Si, and with strict constraints coming from the null results of the XENON100, COUP, PICASSO and LUX experiments (e.g., Bernabei et al. 2008; Aalseth et al. 2014; Aprile et al. 2012; Akerib et al. 2014).

Other point of contention is that, even though the standard cosmological model (Λ-CDM) has proven to be extremely successful in explaining the observed large-scale structure of the universe, there are very relevant inaccuracies in smaller scales. Recent data on low mass galaxies suggests that there is a core-cusp problem: the DM density halo distributions have almost flat cores, in contradiction with the cuspy profile distributions predicted by numerical simulations (e.g., de Blok 2010). The comparison between numerical simulations and observations also seems to suggest that there is a severe overestimation on the number of dwarf satellite galaxies in a given cluster (e.g. Garrison-Kimmel et al. 2013).

Among the possible DM fundamental particles pre-

dicted by current particle physics models, the most studied and well known is the large family of DM particles, known as Weakly Interacting Massive Particles (WIMPs). These particles are characterized for being massive particles and have a very weak interaction (very small scattering cross sections) with baryonic matter. The most popular WIMP is the neutralino – the lightest stable particle in the supersymmetric model (e.g., Bertone et al. 2005). Alternatively, several authors have studied and suggested WIMPs models for which the DM particles present a degree of DM asymmetry identical to the baryonic asymmetry (e.g. Hooper et al. 2004; Iminniyaz et al. 2011; Lopes & Silk 2012). Among other recent review articles about dark matter, the properties of asymmetric dark matter were discussed in detail by Petraki & Volkas (2013); Zurek (2014); Kumar (2014); Kouvaris (2013). The effect of such types of particles were studied in several phases of the stellar evolution (e.g. Kouvaris & Tinyakov 2011a,b; Kouvaris 2012; Casanellas & Lopes 2013), as well as in the context of other astrophysical problems (Feng & Kang 2013). More recently, DM particle physics models have become more rich and complex, a large family of fermion and boson DM particles have emerged, some of which are able to successfully explain the specific features of structure formation in the Universe (e.g., Loeb & Weiner 2011) and simultaneously interpret the DM detection results. Indeed, these WIMP models have become popular because they are able to explain the recent controversial results coming from direct detection experiments (e.g., Cirelli et al. 2013). Such DM models have many features inspired from ordinary baryonic matter, examples are the long range DM interaction (Lopes et al. 2014a; Vincent & Scott 2014) and the magnetic dipole DM (e.g. Sigurdson et al. 2004; Lopes et al. 2014b).

Of the cornucopia of viable DM candidates (e.g., Baer et al. 2014), I am interested in a family of WIMPs arising from the supersymmetric model of particle physics, where the DM particle is generated by an Higgs mechanism (e.g. March-Russell et al. 2008; Baek et al. 2013). This DM particle is created from the kinematic decay of the Higgs boson (e.g. Greljo et al. 2013). In this supersymmetric model it is assumed that any number of Higgs bosons couples with the DM particles through an hidden sector, the so-called Higgs portal by which the DM particle acquires mass. These DM particles have relatively large masses and a very weak interaction with baryons. The mass varies from 100 GeV to 2000 GeV and the scattering cross section is of the order of 10^{-40} cm^2. This DM particle is classified as a scalar, singlet fermion or vector depending of the value of the particle's spin. It is worth to notice that such class of DM particles can, in principle, be detected at the Large Hadron Collider (LHC), in CERN (Baek et al. 2013). In particular, the DM particles generated by the vector Higgs portal do not require the inclusion of stable exotic particles to the extended standard model of particle physics (Pérez & Wise 2013). Without loss of generality, a choice was made to focus this study in this class of DM particles. In the remainder of the paper, this vector Higgs DM is the fiducial WIMP-like symmetric DM particle.

The main goal of this work is to put constraints to DM properties by studying the impact of DM on the evolution of the first generation of low mass stars (Population II stars) formed in primordial dense DM halos.

Stars of Population II are the second generation of stars in the Universe. Such stars are formed from the leftovers of the first generation stars. As the primordial plasma has no content of heavy elements, the first generation of stars formed were very massive and short lived, their rapid termination leads to the formation of the first heavy chemical elements (heavier than helium), like carbon, nitrogen and oxygen. For that reason, the second generation of stars (population II stars) have a low metal content, i.e., a small content in heavy elements. In the present Universe, the low-mass low-metallicity stars due to their long-lifes are the survivors of this primordial stellar population (Salvaterra et al. 2004). The main characteristics of these stars – with numerous star findings, is very well-known in the astronomy community (e.g. Caffau et al. 2012; Christlieb et al. 2012) due to the many photometric and spectroscopic studies of this class of stars. The star SDSS J102915+172927 (also known as Caffau's star) was chosen as the prototype

for this DM study. This well-known star is the oldest star known in our galaxy.

Despite their small scattering cross section with baryonic matter, DM particles can lead to significant (or in some cases drastic) changes in the formation and evolution of stars. There are two mechanisms by which DM can affect the evolution of stars: DM particles provide an additional mechanism for the transport of heat inside the star (e.g., Bouquet & Salati 1989a; Lopes et al. 2002a) or/and DM particles provide the star with an extra source of energy by the self-annihilation of DM particles into standard particles (e.g., Lopes et al. 2011).

The former case is particularly important for stars like the Sun evolving in low density halos. In the case of light DM particles with relatively small scattering cross-sections, the heat transported by DM changes significantly the pulsation spectrum of low order acoustic modes as well as the solar neutrino fluxes, by comparing these theoretical predictions with the observations is possible to constrain the basic parameters of DM particles (e.g., Lopes & Silk 2002, 2010; Taoso et al. 2010; Cumberbatch et al. 2010).

The later case is a very important physical process for stars inside dense DM halos, as stars in the core of galaxies or primordial DM halos. In such scenarios the evolution of the star is modified by the energy generated by the DM annihilation. The study of the evolution of stars in dense DM regions is by now a well established subject with a significant increase of publications in recent years (e.g., Spolyar et al. 2008; Taoso et al. 2008; Iocco et al. 2008; Casanellas & Lopes 2009).

This enlarged abstract is organized as follows: in Sections 2 and 3 I present a description of the energy production mechanism by DM particles annihilation and how the evolution of low mass stars is affected by the presence of dark matter; in Section 4 the constraints in DM properties obtained from formation and evolution of the star SDSS J102915+172927 in a DM halo are studied; in the last Section I discuss the implications of the results for particle physics and cosmology research.

2 Dark Matter Effects on Stellar Evolution

DM particles attracted by the gravitational field of stars travel through their interiors, many of which occasionally scattering off the baryon nuclei encounter on their paths. Although, most of DM particles do not experiment any kind of deflection when travelling across the star, some of them collided a few times with the stellar matter – depending of their DM properties, at each collision the particle loses kinetic energy. If the energy lost by the DM particle is large, the particle ends up being captured by the star, since the velocity of the particle is no longer sufficient to escape the star's gravitational field.

The total number of DM particles trapped inside the star due to the collision with baryons is given by the capture rate Γ_c. In the case of the Sun, this quantity was first estimated by Press & Spergel (1985). This computation was later generalised for massive bodies and main-sequence stars by Gould (1987) and Bouquet & Salati (1989b). In this work, I compute the capture rate as prescribed by equation (2.27) of Gould (1987). A detailed account about how this expression is implemented in the code can be found in Lopes et al. (2011). In a first order approximation this equation takes the form:

$$\Gamma_c = \sum_i \left(\frac{8}{3\pi}\right)^{\frac{1}{2}} \sigma_i \frac{\rho_\chi}{m_\chi} \bar{v}_\chi \frac{x_i M}{A_i m_p} \frac{3 v_{\rm esc}^2}{2\bar{v}_\chi^2} \zeta \qquad (1)$$

where the summation over the subscript i is done for all the chemical species present inside the star, x_i is the relative abundance of the chemical element with the atomic number A_i, σ_i is the DM particle scattering cross section off the nuclei A_i, m_χ is the mass of the DM particle, and ρ_χ and $\bar{v}_\chi$ are the particle density and dispersion velocity of the DM particles in the halo. M and $v_{\rm esc}$ are the total mass and total escape velocity at the surface of the star. As usual $v_{\rm esc}$ is computed as $\sqrt{2GM/R}$ where G, m_p and R are the Newton constant, the mass of the proton and the stellar radius. ζ is a parameter that corresponds to the product of various suppression factors which in the present study can be approximated to unity.

Table 1: DM CAPTURE RATES BY ISOTOPIC ABUNDANCES AT THE BEGINNING OF THE STAR'S EVOLUTION

Isotope	x_i	Γ_c[1] (10^{25}s^{-1})
^{1}H	7.7×10^{-1}	7.4
^{3}He	7.4×10^{-5}	2.1×10^{-7}
^{4}He	2.4×10^{-1}	9.0×10^{-4}
^{12}C	1.8×10^{-7}	2.0×10^{-9}
^{13}C	2.1×10^{-9}	2.6×10^{-11}
^{14}N	5.2×10^{-8}	7.0×10^{-10}
^{15}N	2.0×10^{-10}	2.9×10^{-12}
^{16}O	4.3×10^{-7}	6.6×10^{-9}
^{17}O	1.7×10^{-10}	2.8×10^{-12}
^{29}Si	3.4×10^{-7}	9.5×10^{-9}

This approximate expression is sufficient to evaluate the variation of the DM capture rate with the evolution of the star.

In this work, I take into account the contributions of Hydrogen and Helium, as well as heavier nuclear species that are important for the evolution of population II stars. In Lopes et al. (2011) it is discussed how the different nuclear species contribute to the capture of dark matter by the star, in different stages of stellar evolution in which the chemical compositions are identical to the solar case. Table 1 shows the most relevant of these chemical elements for this study. However, for the limits on the scattering cross sections obtained from the current DM search experiments, in the evolution of low-mass, low-metallicity stars, only the lightest elements, like hydrogen and helium contribute for the capture of DM by the star. During the star's evolution, the capture of DM by scattering off hydrogen and helium dominates over other chemical species. Although the capture by hydrogen is significantly more important than for helium, during the beginning of the evolution (as shown in Table 1), as the star evolves towards more advanced stellar phases, the DM capture by helium increases significantly becoming the dominant capture element in the red giant phase. Therefore, to highlight the leading DM processes affecting the evolution of such class of stars the previous capture rate can be explicitly written for Hydrogen and Helium. Adopting the usual convention for which X, Y and Z represent the mean percentage of Hydrogen, Helium and other elements inside the star, such that $X+Y+Z=1$, the previous approximative capture expression (Equation 1) for hydrogen and helium reads

$$\Gamma_{c,i} = \left(\frac{8}{3\pi}\right)^{\frac{1}{2}} \sigma_i \frac{\rho_\chi}{m_\chi} \bar{v}_\chi \frac{x_i M}{A_i m_p} \frac{3 v_{\rm esc}^2}{2\bar{v}_\chi^2}, \qquad (2)$$

where the subscript i is equivalent to X or Y, x_i is equal to X or Y and σ_i is equal to $\sigma_X = \sigma_{\rm SD} + \sigma_{\rm SI}$ or $\sigma_Y = 16\sigma_{\rm SI}$. In the previous equation for σ_i, $\sigma_{\rm SD}$ and $\sigma_{\rm SI}$ are the spin-dependent (incoherent scattering) and the spin-independent (coherent scattering) scattering cross sections. In the case of the remaining chemical elements, only $\sigma_{\rm SI}$ contributes to the scattering –like for helium, accordingly $\sigma_i = A_i^2 \sigma_{\rm SI}$.

The stellar models computed in these DM evolution scenarios are consistent with results found previously by other authors, see for example Casanellas & Lopes (2009); Fairbairn et al. (2008); Freese et al. (2008); Scott et al. (2009). It is worth noting that in the stellar evolution code used, the capture rate is computed by the numerically integrated equation (2.27) and by all the other related equations from Gould (1987). Nevertheless, the difference found in Γ_c (as shown in Table 1) in relation to the calculation of these authors can be approximately interpreted using equation (2). Typically for a 0.8 $M_\odot$ star evolving in a halo with a density of 10^9 GeV/cm^3, these authors obtained a Γ_c of the order of 10^{33}s^{-1} for a evolved star in comparison with 10^{25}s^{-1} for a star in the beginning of the stellar evolution as shown in Table 1 – a difference of 8 orders of magnitude. This difference is mainly due to the DM parameters chosen in these calculations. For instance, in this case the DM halo density and spin-dependent scattering cross section are 10^6 GeV/cm^3 and 10^{-41} cm^2, respectively, corresponding to a combined order of magnitude 6 times smaller than the ones used in the previously mentioned works. The remaining 2 orders of magnitude difference between the two Γ_c's is related with the fact that for low mass stars evolving within a DM halo for which $\sigma_{\rm SD} \gg \sigma_{\rm SI}$, the Γ_c

increases by 2 orders of magnitude between the beginning of the evolution and its arrival to the main sequence (Lopes et al. 2011).

It's important to highlight that the reason why I am computing stellar models evolving in DM halos with smaller densities than the values used in previous works, results from the fact that the novel method discussed in this work to constrain DM properties, provides quite stringent limits on the values of the DM parameters, as will be discussed in the next sections.

As the DM accumulates inside the star, the total number of DM particles N_χ increases over time. Thus, the variation of $N_\chi(t)$ is given by

$$\frac{dN_\chi}{dt} = \Gamma_c - N_\chi^2 \Gamma_a, \tag{3}$$

where Γ_a is the self-annihilation rate of symmetric DM particles. The solution to this differential equation is (Griest & Seckel 1987):

$$N_\chi(t) = N_0 \tanh\left(\frac{t}{\tau_{DM}}\right). \tag{4}$$

Here $N_0 \equiv \sqrt{\Gamma_c/\Gamma_a}$ is the equilibrium number and τ_{DM} is the time scale for this equilibrium to be reached. In the case of a one solar mass star (as for the stars considered in this study), the steady state is reached in a time scale

$$\tau_{DM} = \frac{1}{\sqrt{\Gamma_a \Gamma_c}} \sim 10\text{yrs}. \tag{5}$$

As τ_{DM} is much smaller than the time-step of the star's evolution, the population of DM particles in the star's core (for most of DM parameters) rapidly reaches equilibrium (equation 3), that is $N_\chi = N_0$, balancing the accretion and annihilation of DM particles (Salati & Silk 1989).

Once the equilibrium is reached (Bertone & Fairbarn 2008), the DM particles accumulated inside the star rapidly enter in thermal equilibrium with baryons, forming a thermal distribution usually called the DM core, with the characteristic radius

$$r_{th} = \left(\frac{9kT_c}{4\pi G \rho_c m_\chi}\right)^{\frac{1}{2}}, \tag{6}$$

where ρ_c and T_c are the central values of the density and temperature of the star, and k_c the Boltzmann constant. The annihilation rate, Γ_a, is taken to be proportional to the WIMP annihilation cross section $\langle \sigma_a v \rangle$ and reads

$$\Gamma_a = \frac{\langle \sigma_a v \rangle}{\frac{4}{3}\pi r_{th}^3}. \tag{7}$$

The pair annihilation of DM particles creates another source in the stellar core. The energy generation rate by DM particles is given by

$$\epsilon_\chi(r) = f_\chi m_\chi n_\chi(r)^2 \rho(r)^{-1} \langle \sigma_a v \rangle, \tag{8}$$

where $n_\chi(r)$ is the number density distribution of DM particles, $\rho(r)$ the stellar density, and f_χ is the fraction of DM particles converted to other particles than neutrinos, and these ones do not contribute to heat the stellar plasma. $n_\chi(r)$ is equal to $N_\chi \pi^{-3/2} r_{DM}^{-3} e^{-(r/r_{DM})^2}$ (e.g., Dearborn et al. 1990; Lopes et al. 2002a). As discussed in the literature, the coefficient f_χ, although of the order of unity can have many different values, depending of the particle physics model and the specific properties of DM annihilation channels. In the case of supersymmetric models, f_χ is of the order of 0.1. As we will see later, this energy production mechanism by DM annihilation can strongly affect the evolution of low mass low metallicity stars, in particular, by producing very significant variations in some stellar observables, like the effective temperature, luminosity and surface gravity, quantities currently measured with precision for the population II stars.

In principle, for these stars, DM particles can also transport energy from the core to the external stellar layers, providing the star with an addition mechanism for the transport of energy, other than convection and radiation (e.g., Bouquet & Salati 1989a; Lopes et al. 2002a). This physical process is also included in the calculations. Nevertheless, as its contribution for the evolution of the star is significantly less important than the DM energy production mechanism, I will treat it as negligible.

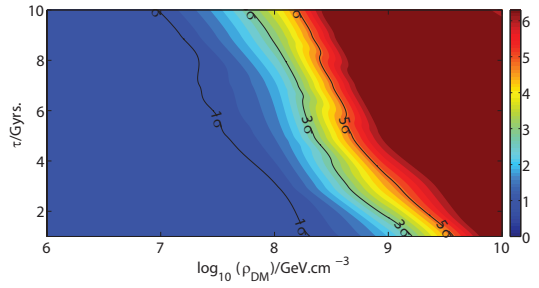

Figure 1: Temporal evolution of the capture rate for a Population II star inside a DM halo. The dashed curves represent the partial capture rates of the two main isotopes: ^{1}H and ^{4}He. The DM halo density is 10^6 Gev.cm^{-3} and the DM particle mass is 500 GeV. The spin dependent cross section is $\sigma_{\rm SD} = 10^{-41}$ cm^2 and the spin independent cross section is $\sigma_{\rm SI} = 10^{-45}$ cm^2.

3 Evolution of low metallicity stars in a dark matter halo

In this study, stellar models (with or without dark matter) are computed using a modified version of the stellar evolution code CESAM (Morel 1997) for which the impact of dark matter in the star's evolution is taken into account following the procedure discussed in Lopes et al. (2011). A detailed discussion about the physical processes related with the impact of dark matter in the evolution of stars and how these processes are implemented in the stellar evolution code can be found in Lopes et al. (2011); Lopes & Silk (2014). CESAM is a well established stellar code being used for several decades by the stellar and solar physics communities to compute models of the Sun and other stars (e.g., Couvidat et al. 2003). In the CESAM code, the evolution of the star at each time step is computed by integrating in space and time, the basic set of stellar structure equations coupled with the network of nuclear reactions. This network is responsible for the stellar nucleosynthesis that determines the changes of the chemical elements and the production of energy inside the star. One of the numerical advantages of CESAM over other stel-

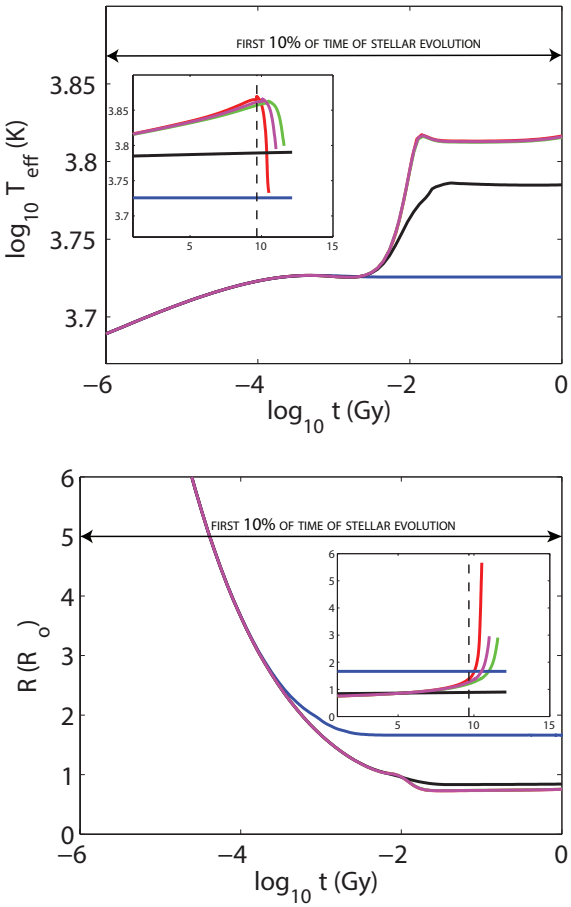

Figure 2: Temporal evolution of effective temperature (i) and radius (ii). The smaller figures represent the temporal evolution of the observables during the remaining 90% of stellar evolution. The red curve corresponds to the evolution of a normal star (no influence of DM). The remaining curves correspond to the evolution of the star inside a DM halo with $m_\chi = 500$ GeV and $\rho_\chi = 10^6$ GeV/cm^3, with spin-dependent cross-section $\sigma_{\rm SD} = 10^{-39}$ cm^2 (magenta curve); $\sigma_{\rm SD} = 10^{-38}$ cm^2 (green curve); $\sigma_{\rm SD} = 10^{-37}$ cm^2 (black curve) or $\sigma_{\rm SD} = 10^{-33}$ cm^2 (blue curve). The dashed line indicates the moment when the red giant phase begins in the normal star.

lar codes is the fact that it uses a variable space-time mesh that adapts at each time step to accurately follow the variations of the different thermodynamical quantities describing the internal structure of the star (Morel 1997). Moreover, CESAM calculates stellar models with a pre-defined numerical accuracy for a variety of physical and numerical assumptions, including different physical data sets (equations of state, opacities tables and nuclear tables), external boundary conditions and numerical scheme of integrations. In this study, I will follow the evolution of the stars of different masses from the pre-main sequence, starting at the moment that the star initiates the gravitational contraction to the main sequence, up to the beginning of the ^{4}He burning in the red giant phase. These stellar models have a chemical composition with a relatively low metallicity content: $10^{-6} \leq Z_\star \leq 0.04$. In this context $Z_\star$ represents the metallicity in each stellar layer.

The present version of the DM stellar code has been used previously to compute the evolution of the Sun and stars in DM halos with different densities: $\rho_\chi \sim 0.38$ GeV cm^{-3} – the low density DM halo of the solar neighbourhood (Lopes et al. 2002a,b; Casanellas & Lopes 2013) or $\rho_\chi \sim 10^6$ – 10^8 GeV cm^{-3} – the high density DM halo in the central region of the Milky Way (Casanellas & Lopes 2009).

In the current study, for the calculation of stars evolving within DM halos, I choose a fiducial DM particle with the mass m_χ in the range of 200 GeV to 2000 GeV (Baek et al. 2013), DM density halo ρ_χ with values between 10^4 cm^{-3} and 10^9 GeV cm^{-3}, $\sigma_{\rm SD}$ with values in the range of 10^{-47} cm^2 to 10^{-37} cm^2, and $\sigma_{\rm SI}$, with exception of Figures 6 and 7, is equal to 10^{-45} cm^2. The scattering cross sections are in agreement with current limits of direct detection experiments (Baek et al. 2013). The annihilation rate $\langle \sigma_a v \rangle$ is equal to 3×10^{-26} cm^{3}s^{-1} from the approximative expression $\Omega_\chi h^2 \approx 3 \times 10^{-27} / \langle \sigma_a v \rangle$ (Scherrer & Turner 1986), where the current observed relic DM density $\Omega_\chi h^2$ is approximately 0.1.

In the following, I compute the present structure of the star SDSS J102915+172927l (our population II reference star) by adopting the same physical prescription found in previous works (e.g., MacDonald et al. 2013). The solar abundances are obtained from Asplund et al. (2005), the initial chemical composition and the metallicity is identical to the one found for the star SDSS J102915+172927 ($Z = 10^{-6}$, the minimum value allowed by the code). The initial helium abundance Y_0 and mixing length parameter α are, respectively, equal to 0.235 and 1.7.

Figures 1 and 2 show the evolution of the capture rate, effective temperature and stellar radius for the star SDSS J102915+172927 evolving in a DM halo. Figure 3 shows the H-R diagram analogue for several stellar models (with and without DM) with a structure identical to the reference star.

4 Dark Matter Effects on the Evolution of SDSS J102915+172927

I will study the effects of DM halos in the evolution of the star SDSS J102915+17292, a low-mass, low-metallicity ($Z \sim 10^{-7}$) Population II star with the observables: effective temperature $T_o = 5881 \pm 150$ K and surface gravity $g_o = (1 \pm 0.5) \times 10^4$ g cm^{-2}. This star is located on the galactic halo, at a distance of 6.2 $\pm$0.2 kpc and is estimated to have an age of 13 Gy, making it one of the oldest stars in our galaxy (Caffau et al. 2012; MacDonald et al. 2013).The star's mass M and luminosity L is obtained by following an identical procedure to the one found in MacDonald et al. (2013). It is important to take into account that there is a discrepancy between the stellar metallicity ($Z \sim 10^{-7}$) and the simulated metallicity ($Z = 10^{-6}$). It will be shown (see Section 4.2) that the differences in the stellar observables that arise from this discrepancy are irrelevant.

4.1 Dark Matter effects on the evolution of a population II star

As discussed in Section 2 and shown in Figure 2, stars evolving within dense DM halos have their evolution strongly altered by the presence of DM in the star's core, as the annihilation of DM particles provides the star with an extra source of energy. The leading pro-

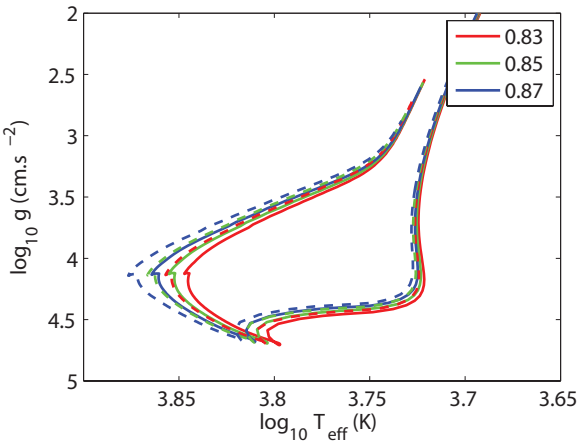

Figure 3: Evolutionary tracks of the stellar models on the $\log T - \log g$ diagram for the star. The solid curves denote evolution in the local universe and the dashed curves track the evolution of the star inside a dense DM halo ($\rho_\chi = 10^6$ GeV.cm^{-3} and $m_\chi = 500$ GeV). The legend tracks the masses by solar units.

cess regulating the impact of DM in the evolution of the star is the DM capture rate. Although equation (2) holds for all chemical elements in any phase of the stellar evolution, as previously mentioned, only the capture rate contributions related with hydrogen and helium is responsible for the presence of dark matter inside the star in any phase of evolution of a population II star. Figure 1 shows how the capture rate changes during the star's evolution. As the star evolves, the capture rate Γ_c reduces significantly, following closely the reduction of the stellar radius of the star. This effect is particularly pronounced in the pre-main sequence during the star's gravitational contracting phase (see Figure 1). Figure 1 also shows the variations of capture rates $\Gamma_{c,X}$ and $\Gamma_{c,Y}$ related with the hydrogen and helium (equation 2). $\Gamma_{c,X}$ is the most important term for almost all the phases of evolution of such stars. Nevertheless, in the red giant phase, due to the significant increase of helium content in the star's core, $\Gamma_{c,Y}$ becomes comparable to $\Gamma_{c,X}$ (see Figure 1). This in part results from the fact that $\Gamma_{c,Y}$ is proportional to $4\sigma_{\rm SI}$ (as in σ_Y).

The presence of DM in the stellar core in some cases alter the stellar structure significantly. Figure 2 shows the variation of effective temperature and radius of the star with time for different DM scenarios. There are two moments in the evolution where the star experiments a drastic change in their structure and consequently in their observables – the beginning of the pre-main sequence and red giant phases (see Figure 2). It is possible to distinguished two distinct DM scenarios for the evolution of the star: *(i)* low DM capture rate (green and magenta curves) – the DM energy source is sub-dominant relatively to the gravity and nuclear energy sources; its impact in the evolution of the star is minor; the slower depletion of hydrogen in the stellar core slightly delays the beginning of the red giant phase without changing significantly the evolution of the star; *(ii)* high DM capture rate (black and blue curves) – the DM energy source is sufficient for the DM to strongly affect the evolution of the star; in some cases the DM energy source stops the gravitational contraction of the star, halting the position of the star in the H-R diagram.

4.2 Dark Matter effects on the stellar observables

Figure 3 shows the evolutionary tracks of the star in the H-R diagram analogue ($\log T - \log g$), where T is the effective temperature and g is the surface gravity of the star. The results are in good agreement with up-to-date estimation of MacDonald et al. (2013). In the case of a star with a mass of 0.85 $M_\odot$, the total luminosity differs only 4% from the estimation of MacDonald et al. (2013). This theoretical prediction is consistent with the observational luminosity determination for which the observational error bar is of the order of 6%.

The evaluation of the DM effects on the evolution of the SDSS J102915+172927 star is done by identifying the variation of T and g in the stellar models relatively to the observable values of T_o and g_o. In order to better estimate the DM impact on these observables, I use the deviation parameter ξ defined as

$$\xi = \sqrt{a\left(\frac{T-T_o}{\delta_T}\right)^2 + b\left(\frac{g-g_o}{\delta_g}\right)^2}, \qquad (9)$$

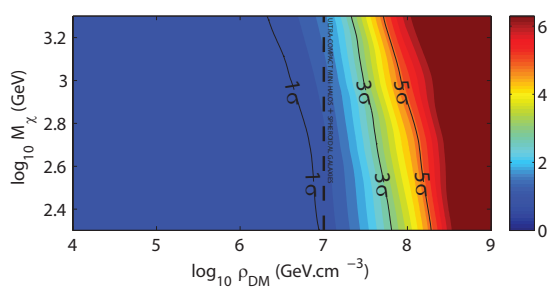

Figure 4: Iso-contours of parameter ξ in the parameter space (m_χ – ρ_χ) for the star SDSS J102915+172927 (in the subgiant phase, at 10.4 Gy). The scattering of DM particle $\sigma_{\rm SD}$ was fixed to 10^{-41} cm^2. The dashed line represents the current lower bounds of ρ_χ for ultra compact mini halos (Yang et al. 2012) and for the spheroidal galaxy Draco (Charbonnier et al. 2011).

where δ_T and δ_g are the observational errors. The quantities a and b are the weights given to each of the observational variables. I choose a and b to be equal to 2/3 and 1/3, as computed from the well-known relations: $L = 4\pi\sigma_\star R^2 T^4$ (where $\sigma_\star$ is the Stefan-Boltzmann constant) and $g = GM/R$. Since ξ is a measure of the deviation of T and g from the observable values T_o and g_o, and the observational errors follow a normal distribution, I can safely exclude all stellar models that are not in agreement with the observational values T_o and g_o. Consequently, I exclude stellar models for which $\xi \geq 3\sigma$ (89%). Such observational analysis is quite robust, since it allows to define well the impact of several DM parameters on the evolution of the star.

Figure 4 shows ξ as a function of m_χ and ρ_χ, for which $\sigma_{\rm SD}$ is fixed to 10^{-41} cm^2 in agreement with current experimental constraints (see Section 1). In principle, stellar DM models for which $\rho_\chi \geq 10^8$ GeV cm^{-3} are excluded, as for these models the DM has a large impact on the star's evolution leading to $\xi \geq 3\sigma$. Charbonnier et al. (2011) estimates the DM density of halos in the dwarf spheroidal galaxy Draco to be in the range 10^7 to 10^9 GeVcm^{-3}. The combination with the results seems to indicate that the DM density is between 10^7 and 10^8 GeVcm^{-3}, as shown in Figure 4. Moreover, these results impose an upper limit to the results of the numerical simulations of Yang et al. (2012) which estimate that the DM densities of ultra-compact mini-halos bigger than of 10^7 GeVcm^{-3}. Additionally, if I fix $\sigma_{\rm SD} = 10^{-45}$ cm^2, as indicated by the more stringent results coming from theoretical particle physics models (Baek et al. 2013), the previous upper bound of ρ_χ increases to 3×10^9 GeVcm^{-3}. These results are in agreement with the numerical simulations of Charbonnier et al. (2011) and still maintain an upper limit on the Yang et al. (2012) results.

Furthermore, the existence of an upper limit to the DM halo density at 10^8 GeVcm^{-3} suggests that if DM particles have the properties discussed in this article, low-mass Population II stars cannot be formed in the central regions of the galaxies, or otherwise these stars will have a very different physical structure. Accordingly, it is expected that, in the very initial phase of galaxy formation, the central core of galaxies should not be an active region of low-mass stellar formation .

Figure 5 shows the variation of ξ with $\sigma_{\rm SD}$ and m_χ, with ρ_χ fix to 10^6 GeV/cm^3 – the value of ρ_χ estimated for the central region of the Milky Way. Repeating the analysis done for Figure 4, I found that only DM models with $\sigma_{\rm SD} \leq 10^{-39}$ cm^2 have a negligible impact in the evolution of the star. This result is in agreement with the upper limit obtained from direct experimental detections for which $\sigma_{\rm SD} \leq 10^{-41}$ cm^2 (e.g. Panci 2014, and reference therein).

Figure 6 shows how ξ varies with both scattering cross sections (spin dependent and spin independent), for which ρ_χ and m_χ are fixed to 10^6 GeVcm^{-3} and 500 GeV. The upper limit $\sigma_{\rm SD} \leq 10^{-39}$ cm^2 found for Figure 5 is still valid, and a new upper limit for the spin independent cross section is found: $\sigma_{\rm SI} \leq 10^{-42}$ cm^2. This last limit is in agreement with results coming from theoretical particle physics models ($\sigma_{\rm SI} \leq 10^{-45}$ cm^2). A thing to notice is that the scattering cross-sections are considered as being independent from each other. This is a consequence of the phenomenological approach used in these calculations (very common method in this type of problems)

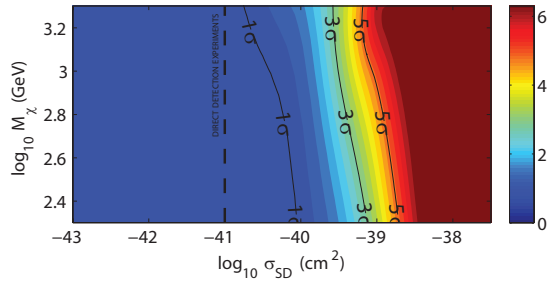

Figure 5: Iso-contours of parameter ξ in the parameter space (m_χ – $\sigma_{\rm SD}$) for the star SDSS J102915+172927 (in the subgiant phase, at 10.4 Gy). The density of the DM halo ρ_χ was fixed to 10^6 GeV cm^{-3}. The dashed line is the current experimental limit for $\sigma_{\rm SD}$.

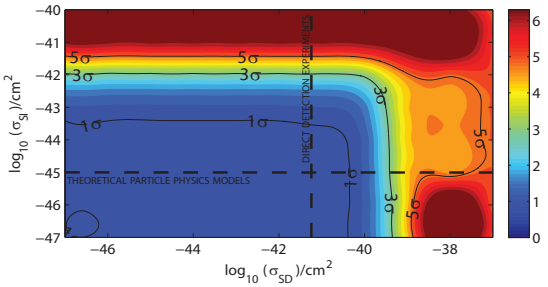

Figure 6: Iso-contours of parameter ξ in the parameter space ($\sigma_{\rm SI}$ – $\sigma_{\rm SD}$) for the star SDSS J102915+172927 (in the subgiant phase, at 10.4 Gy). The density of the DM halo ρ_χ was fixed to 10^6 GeV cm^{-3} and the DM particle mass m_χ was fixed to 500 GeV. The dashed lines represent the current experimental limits for $\sigma_{\rm SD}$ and theoretical limits for $\sigma_{\rm SI}$.

where $\sigma_{\rm SI}$ and $\sigma_{\rm SD}$ are treated as independent quantities. Actually, from a particle physics viewpoint the relation between the spin-dependent and spin-independent scattering cross-sections is not known. Moreover, I observe that this computation is very sensitive to DM halo density ρ_χ (variation of ξ iso-contours in the $\sigma_{\rm SI} - \sigma_{\rm SD}$ as shown in Figure 6). If $\rho_\chi = 10^4$ GeV cm^{-3}, the previous limits for the scattering cross-sections changes to $\sigma_{\rm SD} \leq 10^{-37}$ cm^2 and $\sigma_{\rm SI} \leq 10^{-39}$ cm^2. For even higher DM density halos, these limits become more stringent and may even surpass the current experimental limits. The discovery of a Population II in a high DM density region would thus provide a very interesting constraint to supersymmetric models and direct DM detection experiments.

In order to highlight the complexity of the stellar physics related with the scattering cross-sections of DM particles off baryons (as shown in Figure 6), I compute the ratio $\Delta = \log_{10}(\Gamma_{c,X}/\Gamma_{c,Y}) = \log_{10}(X/Y) + \log_{10}(\sigma_{SD}/\sigma_{SI} + 1) + \log_{10}(1/4))$. The Δ iso-contours are shown in Figure 7. The capture by hydrogen only dominates for DM processes where $\sigma_{\rm SD} >> \sigma_{\rm SI}$, otherwise the capture rate by helium is equally important. These results are in agreement with previous studies of Lopes et al. (2011).

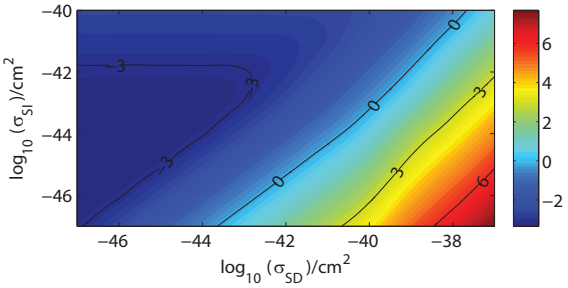

Figure 7: Iso-contours of parameter Δ in the parameter space ($\sigma_{\rm SI}$ – $\sigma_{\rm SD}$) for the star SDSS J102915+172927 (in the subgiant phase, at 10.4 Gy). The density of the DM halo ρ_χ was fixed to 10^6 GeV cm^{-3} and the DM particle mass m_χ was fixed to 500 GeV.

5 Conclusions

Present observational data of population II stars offers a unique way to test DM candidates as proposed by current models of particle physics. In this study, I used the star SDSS J102915+172927 to test the fundamental parameters of Higgs-like (supersymmetric) DM particles. I have shown for the first time that DM halos with a very high density produce very large and visible effects on the evolution of low-mass low-metallicity stars.

These results are of interest for the cosmological numerical simulations community, as such study provides an independent upper limit to the density of DM halos. Current simulations suggest that the density of DM halos where the low-mass stars are formed should have a local DM density below the upper limit 10^8 GeVcm^{-3}, assuming that the other DM parameters are in agreement with current experiment detection limits. Accordingly, low-mass Population II stars can only be formed where the local density is below this upper limit. Thus, for a typical DM density galaxy profile (e.g., Navarro et al. 1996), these stars will start to form only from certain distances from the galactic centre. If no Population II stars are observed in the very central regions of galaxies, that will strong hint in favour of this theoretical model. Equally, by computing DM stellar models for which I fix the density of the DM halo to the value observed in the central region of the Milky Way, I infer the following upper limits to the DM scattering cross-sections: $\sigma_{\rm SD} \leq 10^{-39}$ cm^2 and $\sigma_{\rm SI} \leq 10^{-42}$ cm^2.

Although, population II stars like the star SDSS J102915+172927 are currently located in regions of the Universe with a relatively low DM density, very likely these very old stars were formed within the high density DM halos of the primordial universe. In fact, these low-metallicity stars experiment their most significant structural changes during a short time period in the beginning of the pre-main sequence phase. Therefore, it is reasonable to assert that the DM will have a major impact on the star's structure during this phase.

Comparatively DM has a relatively smaller effect during the long and slow passage of the star along the main sequence phase, where it is known that the star's structure does not change very much. Only when the star enters in the red giant phase the star structure experiments again important changes, and hence the DM impact will become more significant from this stage. As predicted by several cosmological simulations, primordial DM halos (with high densities) are very likely the birthplaces of low mass low-metallicity stars, for which, accordingly to my simulations, the DM particles should affect significantly their formation. Using the observational data for the star SDSS J102915+172927 it is expected that the DM density of the primordial halo should not be larger than 10^8 GeVcm^{-3}, assuming that the DM halo is constituted by Higgs Portal DM particles.

Nevertheless, this initial study has some important caveats to be noted: I do not consider the time evolution of the density of the DM halo and the variation of the location of the star inside the DM halo, which would influence significantly the impact of DM in the star; Equally, in this first study I have concentrated on a specific set of DM models: the extension of this analysis to other DM models should reduce significantly the family of DM particle candidates in agreement with observations. Additionally, in order to keep my results as conservative as possible, I decided not to take into consideration effects such as DM evaporation and WIMP self-interaction. Finally, the study of Population II stars in DM halos of high density, as found in spheroidal galaxies, can provide another independent complementary test of the class of DM particle models.

The population of low-mass low-metallicity stars provides a unique and novel way to independently test the DM particle results obtained either from the many particle physics model predictions of the current controversial data found by the experimental direct detections. This type of stellar analysis could be strongly improved as the data of stellar missions, such as GAIA (Perryman et al. 2001), which is providing a detailed analysis of the map of stars in our own galaxy, becomes available.

References

Aalseth C.E. et al. (CoGeNT Collab.), 2014, arXiv:1401.6234

Akerib, D.S. et al. (LUX Collab.), 2014, Phys. Rev. Lett., 112, 091303

Aprile, E. et al. (XENON100 Collab.), 2012, Phys. Rev. Lett., 109, 181301

Asplund, M. et al. in *Proceedings of the Cosmic Abundances as Records of Stellar Evolution and Nucleosynthesis in honor of David L. Lambert, San Francisco, 2005* edited by Barnes III, Thomas, G. and Bash, F. N. (2005)

Baer, H. et al. 2014, arXiv:1407.0017

Baek, S. et al., 2013, JHEP, 2013, 36

Bernabei, R. et al. (DAMA Collab.), 2008, EPJC, 56, 333

Bertone, G. and Fairbarn, M., 2007, Phys. Rev. D, 77, 4

Bertone, G. et al., 2005 Phys. Rep., 405, 279

Bertone, G., 2010, Nature, 468, 389

Bouquet, A. and Salati, P., 1989a, ApJ, 346, 284

Bouquet, A. and Salati, P., 1989b, A&A, 217, 270

Caffau, E. et al., 2012, A&A, 542, A51

Casanellas, J. and Lopes, I., 2009, ApJ, 705, 135

Casanellas, J. and Lopes, I., 2013, ApJL, 765, L21

Charbonnier, A. et al., 2011, MNRAS, 418, 1526

Christlieb, N. et al., 2012, Nature, 410, 904

Cirelli, M., Del Nobile, E., & Panci, P. 2013, JCAP, 1310, 019

Couvidat, S. et al., 2003, ApJ, 599, 1434

Cumberbatch, D. T. et al., 2010, Phys. Rev. D, 82, 103503

Dearborn, D. et al., 1990, ApJ, 354, 568

de Blok, W., 2010, Adv. Astron., 2010, 789293

Fairbairn, M., Scott, P. & Edsjö, J.,2008, Phys. Rev. D, 77, 047301

Feng, L., & Kang, Z. 2013, JCAP, 10, 008

Freese, K. et al., 2009, ApJ, 693, 1563

Freese, K., Spolyar, D. & Aguirre, A., 2008, JCAP, 11, 014

Garrison-Kimmel, S., 2013, MNRAS, 433, 3539

Gould, A., 1987, ApJ, 321, 571

Greljo, A. et al., 2013, JHEP, 2013, 190

Griest, K. and Seckel, D., 1987, Nuc. Phys. B, 283, 681-705

Hooper, D. et al., 2004, Phys. Lett. B, 605, 228-236

Iminniyaz, H., Drees, M., & Chen, X. 2011, JCAP, 07, 003

Iocco, F. et al., 2008, MNRAS, 390, 1665

Kouvaris, C. 2013, arXiv:1308.3222

Kouvaris, C. 2012, Phys. Rev. Lett., 108, 191301

Kouvaris, C. & Tinyakov, P. 2010, Phys. Rev. D, 82, 63531

—. 2011a, Phys. Rev. D, 83, 083512

—. 2011b, Phys. Rev. Lett., 107, 91301

Kumar, J. 2014, AIP Conf. Ser., 1604, 389

Loeb, A. & Weiner, N. 2011, Phys.Rev.Lett., 106, 171302

Lopes, I. and Silk J., 2002, PRL, 88, 151303

Lopes, I. and Silk J., 2010, Science, 330, 462

Lopes, I. and Silk J., 2012, ApJ, 757, 130

Lopes, I. and Silk J., 2014, ApJ, 786, 25

Lopes, I. et al., 2002a, MNRAS, 337, 1179

Lopes, I. et al., 2002b, MNRAS, 331, 361

Lopes, I. et al., 2011, Phys. Rev. D, 83, 063521

Lopes, I., Panci P. & Silk J. 2014,ApJ, 795 162.

Lopes, Kadota K.& Silk J., 2014, ApJL, 780, L15.

Navarro J. F., Frenk C. S., White S. D. M., 1996, ApJ, 462, 563

MacDonald, J. et al., 2013, MNRAS, 421, 1425

March-Russell, J. et al., 2008, JHEP, 2008, 58

Morel, P., 1997, A&A, 124, 597

Panci, P., 2014, arXiv 1402.1507

Pérez, P.F. and Wise, M.B. 2013, JHEP, 2013, 94

Petraki, K., & Volkas, R. R. 2013, Int.J.Mod.Phys., A28, 1330028

Perryman, M. A. C. et al., 2011, A&A, 369, 339

Press, W. H. and Spergel, D. N., 1985, ApJ, 296, 679

Salati, P. and Silk, J., 1989, ApJ, 338, 24

Salvaterra, R. et al., 2004, New Astron., 10, 113

Sigurdson, K. et al., 2004, Phys. Rev. D, 70, 083501

Spolyar, D. et al., 2008, Phys. Rev. Lett., 100, 051101

Scherrer, R. J., & Turner, M. S. 1986, Phys. Rev. D, 33, 1585

Scott, P., Fairbairn, M. & Edsjö, J., 2009, MNRAS, 394, 1

Taoso, M. et al., 2008, Phys. Rev. D, 78, 123510

Taoso, M. et al., 2010, Phys. Rev. D, 82, 083509

Yang, R. et al., 2012, JCAP, 2012, 23

Yoon S.-C. et al., 2008, ApJ, 688, L1

Vincent, A. C., & Scott, P. 2014, JCAP, 4, 019

Zurek, K. M. 2014, Phys. Rep., 537, 91